Overview of JET Results

M. L. Watkins 1) on behalf of JET EFDA Contributors[1]

1) EFDA-JET Close Support Unit, Culham Science Centre, Abingdon, OX14 3DB, UK and
EURATOM-UKAEA Fusion Association, Culham Science Centre, Abingdon, Oxon OX14 3DB, UK.
e-mail contact: michael.watkins@jet.efda.org

Abstract. The development for ITER of integrated operating scenarios with acceptable first wall power loadings and high fusion power has gained urgency in view of JET's intent to install an ITER-like beryllium wall, tungsten divertor and major heating system upgrades. Since the last IAEA Conference the understanding of key issues has progressed with recent analyses of past results and the first results from the 2006 Experimental Campaigns, which exploit new enhancements, extending operation to highly shaped, high power plasmas with an improved diagnostic capability. Issues related to the core plasma performance include global energy confinement, temperature profile stiffness, toroidal momentum transport, density peaking, impurity accumulation, core MHD and fast ion effects. Active control of the local current profile is seen as a means to improve performance by modifying MHD and transport effects. Issues related to the edge plasma include the erosion of plasma facing components caused by high power loadings that result from edge MHD instabilities which must be ameliorated, and edge material migration which can influence fuel retention and inventory. The need to resolve these issues re-enforces the need to test ITER wall materials under high performance conditions, as foreseen in the longer-term JET programme in support of ITER.

1. Introduction

Since the last IAEA Conference [1], JET has upgraded its divertor, heating systems and diagnostics, extended the analysis of past results, started its 2006 Experimental Campaigns and progressed the understanding of key issues related to the qualification for ITER of integrated operating scenarios with acceptable fusion power and first wall power loadings. The first key issue, addressed in Section 2, is the performance of the ITER baseline scenario [2] and the more advanced scenarios which offer potential for improved performance. Emphasis is given to coordinated multi-machine experiments on global energy confinement, density peaking and temperature profile stiffness, together with specific JET experiments on electron heat transport (using Ion Cyclotron Resonance Heating (ICRH) to modulate the electron temperature), impurity accumulation (expected with neoclassical transport), and momentum transport (in view of its potential role in stabilising turbulence). The important role of the plasma current profile in influencing plasma performance is becoming increasingly recognised, and JET uses Ion Cyclotron Current Drive (ICCD) and Lower Hybrid Current Drive (LHCD) to provide active control of the local current profile to control MHD activity and transport losses, thereby enhancing performance. The second key issue, addressed in Section 3, is that of achieving acceptable wall power and particle loadings in conjunction with high fusion performance. The ELMs associated with the ITER baseline scenario will cause erosion and damage to plasma facing components and it is essential to develop towards scenarios with more benign ELMs. Furthermore, it is essential to chart the migration paths of material eroded from these components, since this will impact on fuel retention and inventory. The resolution of all these issues has gained urgency in view of JET's near-term intent to install an ITER-like beryllium wall and tungsten divertor [3, 4] for which the related R&D is reviewed in Section 4. The ITER-like wall, together with further upgrades to the ICRH and Neutral Beam (NB) systems, aims to confront the dual challenges of improved core plasma performance and acceptable first wall power and particle loadings required for ITER, providing a test-bed for high power integrated scenarios at the most ITER-relevant parameters with a combination of ITER-like wall materials.

[1]See Annex

2. Core plasma performance

2.1. Global energy confinement

In global terms plasma performance in the ITER baseline scenario (H-mode with MHD instabilities in the core (sawteeth) and in the edge (Edge Localised Modes, ELMs)) is measured by the thermal energy confinement time which is often expressed in terms of the IPB98(y,2) empirical scaling [5]. However, this scaling can be optimistic as density is increased towards the Greenwald density, and can be overly pessimistic with respect to its dependence on normalised plasma pressure, β. Dedicated identity experiments with matched dimensionless parameters on JET and C-MOD show collisionality, ν^*, rather than the Greenwald density fraction, F_g, to be the relevant dimensionless parameter. However, dedicated ν^* scans on JET, DIII-D, JT-60U, COMPASS-D and C-MOD show that the ν^* dependence is not well-represented by a simple power law. Furthermore, dedicated β-scans on JET an DIII-D show no dependence of confinement on β while JT-60 data show a β-degradation weaker than that of IPB98(y,2). These observations from multi-machine dimensionless transport experiments are found to be better described by a two-term scaling in which the β and ν^* dependencies are stronger in the contribution made by the pedestal energy than the core plasma energy [6]. None-the-less, the two-term scaling is no better than IPB98(y,2) at describing the fall in confinement with increasing density.

2.2. Stiff temperature profiles close to threshold

Temperature profiles often reveal critical thresholds in the temperature gradient scale length, R/L_T, which, together with high thermal diffusivities, maintain stiff temperature profiles, close to the thresholds. Electron heat transport studies at low collisionality on JET use Ion Cyclotron Resonance Heating (ICRH) to modulate the electron temperature, T_e, to determine the degree of stiffness and threshold in R/L_{Te}, and to allow comparison with other tokamaks [7, 8]. Thresholds are found to be in broad agreement with theoretical predictions for TEM instabilities from linear gyrokinetic codes (GS2, KINEZERO). Stiffness levels are found to be higher in JET and increase with temperature, implying that the higher temperatures expected in ITER will be determined closely by the thresholds. Ion temperature stiffness studies have also started on JET with upgraded Charge Exchange Spectroscopy (CXS) with improved time resolution.

A broad range of steady-state and perturbative transport observations can be simulated by 1-D first-principle-based transport models (such as the Weiland model and GLF23), but these can fail under particular operational conditions. Comparison between experiment and non-linear 3-D turbulence codes (fluid: TRB and CUTIE, gyrokinetic: GYRO) have provided significant physical insight, but these codes are not yet reliable predictive tools. In particular, all models have failed so far to reproduce, at the same time, the propagation of very fast cold T_e pulses from the plasma edge and T_e modulations. Models featuring turbulence spreading seem to have better capabilities to match both modulation and cold pulse data, but need a more thorough assessment [9].

2.3. Low core toroidal momentum transport

Global and local toroidal momentum transport has been studied using a large database of ELMy H-mode discharges (most of which are dominated by ITG turbulence), local transport analysis and predictive transport simulations. The ratio of the global energy confinement time to the momentum confinement time is found to be close to unity, except for low density discharges where the ratio is 2–3 [10]. On the other hand, local transport analysis of some tens of discharges under different plasma conditions shows that the Prandtl number (the ratio of toroidal momentum and ion heat diffusivities, χ_ϕ/χ_i) lies in the range $0.1<\chi_\phi/\chi_i<0.4$, that is with the Prandtl number being significantly smaller than unity, the value often associated with ITG turbulence. Predictive transport simulations also confirm that $0.1<\chi_\phi/\chi_i<0.4$ reproduces well the core toroidal velocity profiles [10]. The apparent discrepancy

between global and local estimates of the ratio between momentum and ion heat transport can be explained by momentum confinement in the edge pedestal being worse than ion heat confinement. Concerning stiffness, while temperature profiles exhibit critical thresholds in R/L_T, the toroidal velocity profile does not show a threshold in R/L_v. While these experimental and modelling results render the assumption $\chi_\phi/\chi_i \sim 1$ unjustified for ITER predictions, further experiments and theory are required before firm extrapolations to ITER can be made.

2.4. Density peaking

The peakedness of the density profile, $n_{e0}/\langle n_e \rangle$, will affect overall plasma performance. Evidence for increasing peaking with decreasing effective collisionality, ν_{eff}, has been found by statistical analysis of a combined JET and ASDEX Upgrade database of ELMy H-mode discharges (Fig. 1) [11, 12]. This reduces co-linearities with F_g and the fuelling source, and confirms ν_{eff} as the most relevant parameter for density peaking. Although wall and NB injected neutral sources contribute to density peaking [13], these and the neoclassical Ware pinch are insufficient to explain all the experimental data, and the existence of a turbulence-driven particle pinch is required. This is in line with theory predictions of curvature and thermo-diffusion pinches, although quantitative agreement with gyrokinetic estimates of the dependence on ν_{eff} is still under assessment. Density peaking is found to persist even under conditions of strong central electron heating in both JET and TCV, that is, TEM-induced outward thermo-diffusion does not appear to be sufficient to overcome the inward pinch. The empirical scaling deduced from multiple regression analysis predicts $n_{e0}/\langle n_e \rangle$ above 1.3 for ITER, thereby counteracting the negative consequences of a lower than expected density limit [14] but increasing the likelihood of impurity accumulation.

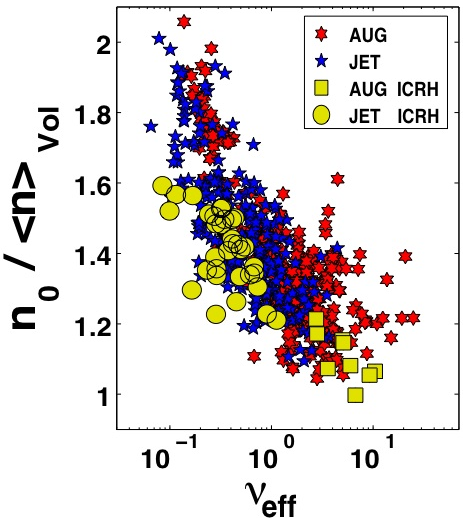

FIG. 1. Multi-machine data showing increasing density peaking with decreasing effective collisionality, ν_{eff}, which is $6x10^{-2}$ for ITER.

2.5. Impurity accumulation

A concern with peaked density profiles is the concomitant accumulation of impurities expected with neoclassical transport. However, experiments on JET show that impurity transport is anomalous, even for high Z impurities [15]. Ion Cyclotron Resonance Heating (ICRH) experiments have suggested the possibility of controlling high Z impurity accumulation using electron heating [16]. With dominant ^{3}He minority ion heating (MH), Ni is found to accumulate in JET with an inward pinch, which is an order of magnitude larger than the neoclassical value. On the other hand, with dominant ^{3}He mode

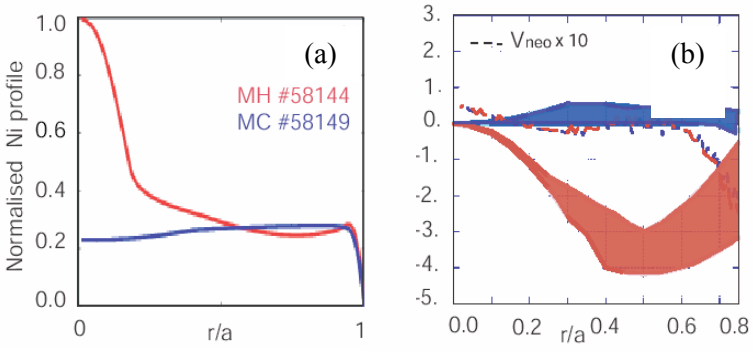

FIG. 2. (a) Ni impurity density profiles and (b) convection coefficient profiles with ICRF minority heating (MH; red), and mode conversion (MC; blue). With MC heating, the Ni accumulation in the core is reduced greatly.

conversion electron heating (MC), the pinch is outward and the diffusion is higher, preventing accumulation (Fig. 2). This is in line with gyrokinetic stability calculations (GS2) which show that for a plasma dominated by ITG turbulence, as is the case for ion MH, the pinch is inwards, while R/L_{Te}-driven TEM instabilities would contribute to an outward pinch with MC electron heating. A novel type of pinch, in addition to curvature and thermo-diffusion, associated with parallel velocity fluctuations, has been found to be responsible of such behaviour [17]. These results suggest the possibility of impurity control with dominant electron heating, as expected from α-particles in a burning plasma. Furthermore, turbulence-driven anomalous pinches and diffusion are expected to have dependences on charge, Z, and mass, whose match with JET experimental results is under assessment. The impurity peaking factor at mid-radius is expected to vary with Z at low Z, due to thermo-diffusion, with a saturation at high Z. This is in accord with experiment, and differs from neoclassical predictions of increasing impurity peaking with Z [16].

2.6. Sawtooth triggering and fast ion physics

The regular occurrence of core MHD instabilities (sawteeth), when the central safety factor, q_0, falls below unity, can flatten profiles and remove high Z material and ^{4}He ash which might otherwise accumulate in the core. Therefore, it is essential to understand the triggering of sawtooth crashes which often follows the occurrence of core-localised Toroidal Alfvén Eigenmodes (TAEs; so-called "tornado modes") driven by ICRH fast ions. These modes expel fast ions from within the q=1 surface into the outer plasma as well as onto the first wall, leading to a loss of fast ion stabilisation of the sawteeth and a large sawtooth crash. Between crashes, particle losses are characterised by a broad distribution in pitch angle and Larmor radius, as evidenced on JET by a new fast ion loss scintillator detector [18]. During the sawtooth crash, the lost particles are confined to a narrow range in pitch angle at a lower energy but with larger amplitude (Fig. 3). These observations are interpreted, in the former case, as fast ion losses induced by tornado modes [19] and fishbones, and in the latter case as the expulsion by the sawtooth of ICRH-accelerated ions. Co- and counter-current propagating tornado modes have also been observed on JET for the first time (Fig. 4). The drive for these modes is considered to come from the anisotropy of the ICRH-accelerated fast ion distribution rather than the pressure gradient [20]. The time evolution of some of these modes also provides indications that the magnetic shear may be weakly reversed.

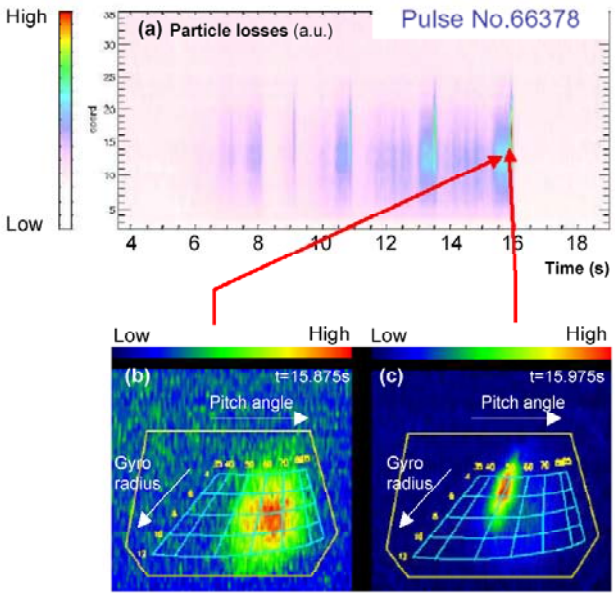

FIG. 3. Scintillator probe data showing difference in distribution of fast particles in Larmor radius (energy) and pitch angle, arriving at the first wall (a) between and (b) during a sawtooth crash.

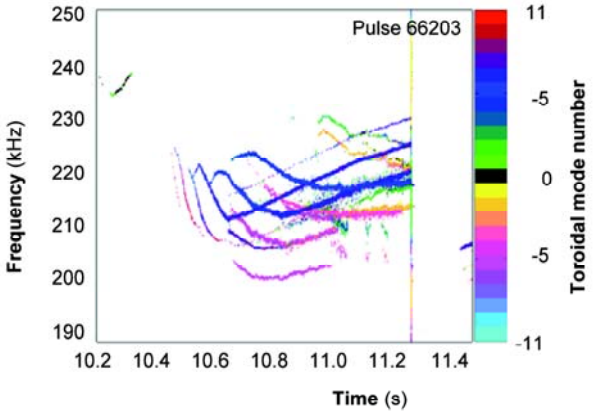

FIG. 4. Tornado modes observed with magnetic diagnostics. The existence of positive and negative toroidal mode numbers shows mode propagation in the co- and counter-current directions.

2.7. Sawtooth and NTM control using local current profile control

To realise the benefits of peaked profiles, sawtooth control is essential to avoid large sawteeth which destabilise neoclassical tearing modes (NTMs) that can lead to a deterioration of plasma confinement and even initiate disruptions. Such control has been achieved on JET by raising the local magnetic shear at the q=1 surface above a critical threshold for triggering sawteeth, in line with analysis [21, 22]. Calculations of localised ion cyclotron current drive (ICCD) using the SELFO code (full wave code with a 3-D Monte Carlo solver for the orbit-averaged Fokker-Planck equations) show a significant increase in the magnetic shear near the q=1 surface for 2.7T/2.6MA JET experiments which demonstrate the active control of sawteeth. ICCD at 47MHz with counter-current propagating waves near q=1 on the high field side is used to increase the local magnetic shear and destabilise sawteeth which had been stabilised by fast particles during central MH at 42MHz with a low (~5%) concentration of H in D [23]. These results show promise for the avoidance of NTMs in JET and ITER H-modes, which are always in a regime above the NTM marginal stability threshold. Initial results from JET also indicate that pre-emptive application of Lower Hybrid Current Drive (LHCD) can raise the threshold for triggering m=2, n=1 NTMs induced by error fields, and can suppress partially pre-existing m=3, n=2 NTMs. The appeal of such control has been strengthened by EDGE2D modelling of the JET scrape-off layer (SOL) in ELMy H-mode discharges when gas puffing near the LH launcher leads to an increase of n_e in front of the LH launcher (to above the cut-off density, $1.7 \times 10^{17} m^{-3}$ at 37GHz), thereby allowing good RF coupling with a large plasma-launcher separation (~0.10m), comparable to that expected in ITER. Under these conditions, the SOL n_e profile is reproduced, provided the gas puff (10^{22}/s) and LH power deposition in the SOL (~15kW, or 0.05% of the total LH power) are sufficiently large to increase T_e, ionisation, and n_e in the far SOL [23].

2.8. Improved H-mode performance with current profile control

Better performance than the ITER baseline scenario can often be achieved by active control of the current profile. On JET, LHCD is also used extensively to drive current and maintain q_0 above unity to prevent sawteeth and the large NTMs which they can trigger. As a result, the normalised plasma pressure, β_N, in the central core of such an hybrid mode (or improved H-mode) is higher than for the ITER baseline scenario, although high edge pedestal energies and Type I ELMs can still persist. Transport simulations show that current profile control and off-axis current drive is needed to maintain q_0 above unity for a hybrid scenario in ITER [24].

JET experiments show that with q_0 above unity, weak central magnetic shear and edge q_{95}~4, sawteeth are absent and energy confinement is higher than expected from the IPB98(y,2) scaling, but consistent with the weaker β-dependence found in dedicated confinement scans in JET and DIII-D. The analysis of a newly assembled database of ~100 JET hybrid discharges shows improved core confinement in some cases, with high $T_i(0)$~17keV and $T_e(0)$~8keV, short temperature gradient scale lengths (R/L_{Ti}>14 and R/L_{Te}>11) over a wide region (Δr~0.2m) in the plasma core, with a sharp decrease in both χ_i and χ_e over the entire plasma core for more than 5s. This is reminiscent of the Internal Transport Barriers (ITBs) found in plasmas with reversed central magnetic shear. While the pedestal temperature, T_{eped}~4keV is quite high and the pedestal density, $n_{eped} \sim 1.3 \times 10^{19} m^{-3}$ is quite low, these plasmas exhibit little (possibly Type III) or no ELM activity, even though the power input is well above both the L-H threshold and that required to access Type I ELMs. This behaviour occurs in discharges with relatively low density and results in global performance comparable to that in standard hybrid discharges with Type I ELMs (β_N~2, H_{98}~1, $\beta_N H_{98}/q_{95}^2$~0.13), with 37% and 23% of the plasma stored energy residing in the pedestal and in the core, respectively, together with a 40% non-thermal contribution [25].

2.9. Improved performance with current profile control and ITBs

LHCD is also used on JET to provide deep shear reversal with an off-axis minimum in the safety factor, q_{min}, which is favourable for the formation of an ITB. In this magnetic configuration, an ITB is often observed as a well-localised narrow layer with low heat diffusivity. This is confirmed by the propagation of T_e modulations using MC ICRH both inside and outside the ITB (Fig. 5). These indicate that ITBs are regions of improved confinement, which exhibit a lack of stiffness and sub-critical transport, that is well below threshold [26]. On JET, the formation of an ITB appears to be associated with the short-lived depletion of rational surfaces in the core plasma [27]. This occurs in the vicinity of q_{min} when q_{min} is just above an integer value, as indicated by O-mode interferometry measurements which show that Alfvénic waves at the magnetic shear reversal point, known as Alfvén Cascades (ACs), are suppressed for a brief period as the decreasing q_{min} during the early phase of the discharge approaches an integer value. The suppression of ACs is correlated in time with the appearance of an ITB as seen, for example, on the T_e profiles obtained by ECE. This has been demonstrated for densities up to $4.1 \times 10^{19} m^{-3}$ in NB heated discharges and $5.2 \times 10^{19} m^{-3}$ in discharges fuelled also with deuterium pellets. Similar observations of ITB triggering events and ACs have been made on DIII-D [28].

While ITB triggering due to rarefaction of rational surfaces of the q-profile has a robust basis, the mechanisms governing the subsequent dynamics and sustainment of the ITB are less clear. The role of negative magnetic shear has been reported extensively in JET [29]. Another key mechanism to stabilise turbulence is the ExB shear flow, and experimental measurements on JET with CXS show that the poloidal velocity of carbon ions can be an order of magnitude above the neoclassical value within the ITB (Fig. 6) [30]. This increases significantly the derived radial electric field and the E×B flow shear. When the experimental poloidal velocity is used in predictive transport simulations (such as the Weiland model), the onset, location and strength of the ITB is reproduced well, while it is not when the neoclassical poloidal velocity is used [31]. The most plausible explanation for the observed anomalous poloidal velocity is turbulence-driven poloidal flows. Both the TRB and CUTIE turbulence codes produce anomalous poloidal velocities, significantly larger than neoclassical values [10]. A crucial question yet to be resolved is the causal relation between the anomalous poloidal velocity and the onset of the ITB.

Recently, Advanced Tokamak (AT) discharges with ITBs have been studied

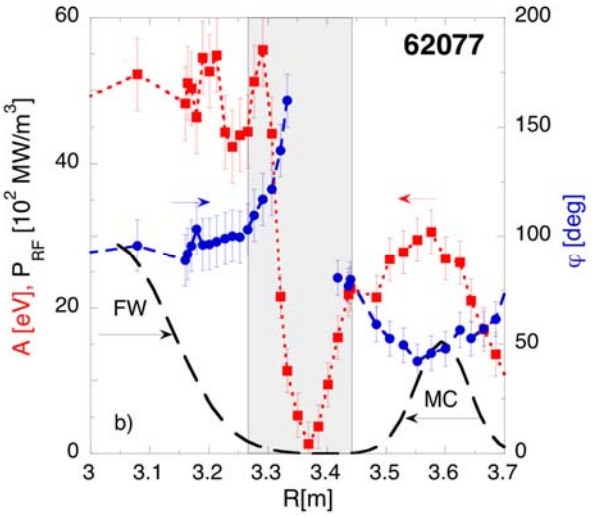

FIG. 5. Amplitude (red) and phase (blue) of a propagating heat wave in a JET discharge with an ITB, showing the ITB as a narrow layer with reduced heat diffusivity.

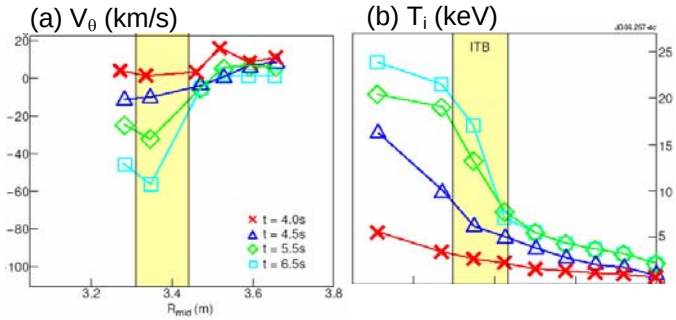

FIG. 6. (a) Poloidal velocity profile and (b) ion temperature profile during the development of an ITB, showing that the poloidal velocity at the ITB reaches ~60km/s, significantly higher than neoclassical values.

in conditions closer to ITER, in two new configurations (LUD and ITER-AT) which take advantage of the upgraded heating power and new divertor on JET (Fig. 7). The LUD configuration has a low upper triangularity, δ_U~0.2, but a high lower triangularity, δ_L~0.55, and the ITER-AT configuration has high upper and lower triangularities of δ_U~0.45 and δ_L~0.55, whereas previous AT discharges on JET were studied mainly in a configuration with a low triangularity of δ~0.3. The LUD configuration was studied with high heating power (27MW, comprising 20MW of NB, 5MW of ICRH and 2MW of LHCD) and an ITER-relevant q_{95}~5 at 1.9MA/3.1T, compared with q_{95}~7.5 previously at low δ~0.3. Under these conditions, ITBs were established with simultaneously high pedestal and core densities (n_{eped}~2.5x10^{19}m^{-3} and n_{eo}~6x10^{19}m^{-3}) relative to those obtained previously at low δ~0.3, with T_{io}~8-10keV close to T_{eo}~7-8keV, and with ELMs which do not affect the ITB (T_{eped}~1.1-1.3keV with 80Hz Type I ELMs, compared with T_{eped}~2-3keV and n_{eped}~1.5x10^{19}m^{-3} with similar frequency Type III ELMs, previously at low δ~0.3) (Fig. 8). At peak performance the non-inductive current fraction reached 70%. A non-monotonic q profile was sustained for ~4s [32]. In the present experimental campaigns, the q and temperature profiles will be controlled simultaneously, using advanced real-time algorithms to take account of two different time-scales (confinement and current diffusion times) [33]. Predictions have also been made for the planned power upgrade to ~45MW on JET. If confinement in the Advanced Scenario were to scale as IPB98(y,2), but with an enhancement factor increasing with increasing power to a value of 1.5 at 45MW, it would be possible for JET to access conditions of full current drive under stationary conditions at high current (2.5MA) and high density (n_l~5x10^{19}m^{-3}), in a regime in which fusion performance increases with increasing bootstrap current fraction [32].

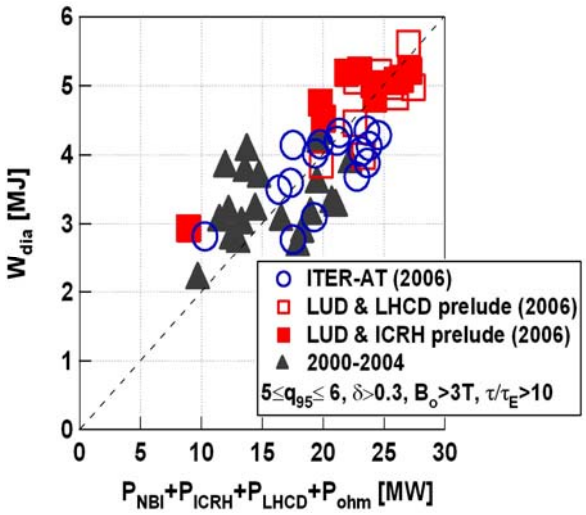

FIG. 7. Progress in increasing performance in JET AT discharges, including recent results following power upgrades and the installation of a new divertor for high triangularity operation.

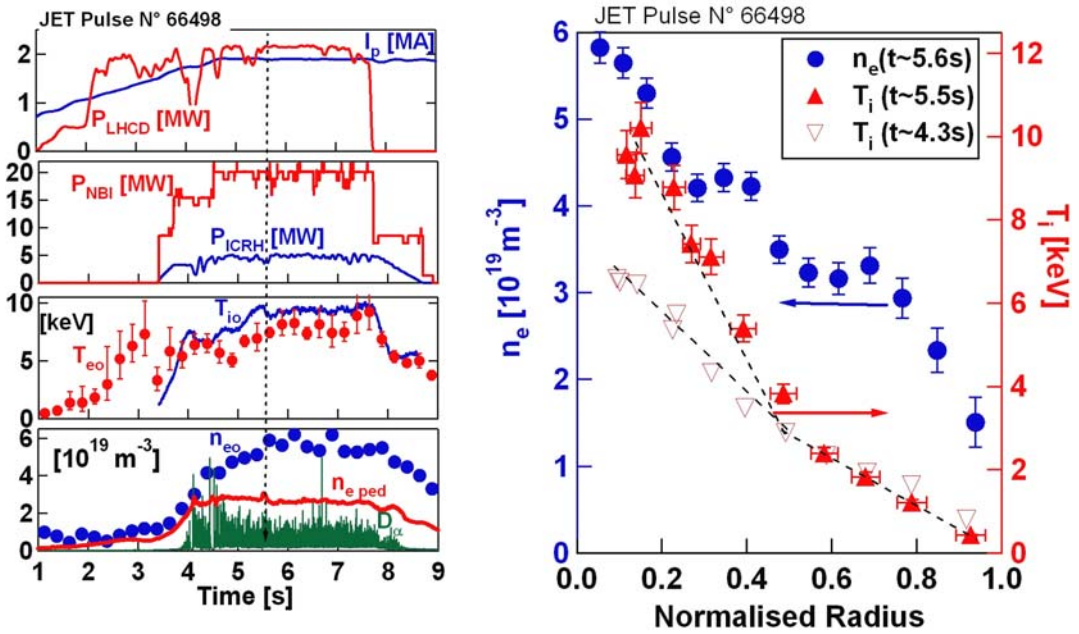

FIG. 8. (a) Time traces of an Advanced Tokamak discharge in the LUD configuration and (b) density and temperature profiles close to the time of peak neutron rate (closed symbols) and, as a reference, the temperature profile prior to ITB formation (open symbols).

Alfvénic activity is readily excited in AT discharges. Following the installation of new low-attenuation waveguides, which yield a 20dB enhancement in signal-to-noise ratio, the first spatially localised measurements of ACs in the JET plasma core have been obtained using multi-channel X-mode reflectometry [34] (Fig. 9). Together with precisely calibrated NB injection velocities (v_b), these measurements indicate for the first time that the velocity threshold for the excitation of Alfvén instabilities, in particular ACs, can be much lower than observed previously, and is in the sub-Alfvénic range $0.1<v_b/v_A<0.3$. This suggests that a significant interaction may occur between Alfvénic modes and nearly thermalised α-particles in a reactor. Studies on an AT configuration for ITER have also begun and optimisation will continue during 2006/7, with multi-channel X-mode reflectometry providing a valuable tool for AT discharge optimisation by tailoring the q profile, with the aim of maximising the radius at which the ITB forms [34].

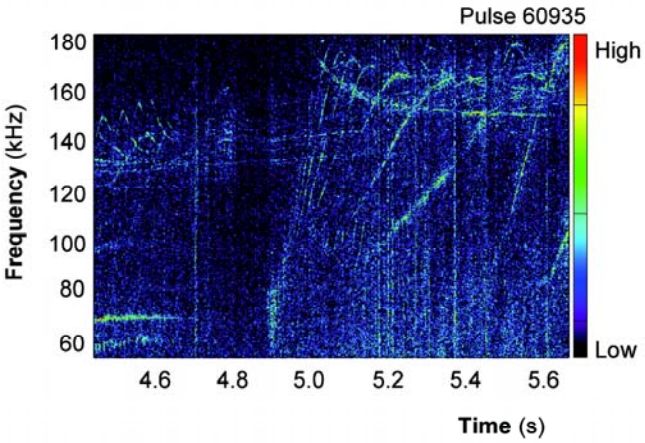

FIG. 9. Alfvén cascades observed with the X-mode reflectometer, using new low-attenuation waveguides.

2.10. Performance limitation by Resistive Wall Modes

In AT operation, plasma performance will be limited, ultimately, by resistive wall modes (RWMs) as β_N aproaches the ideal wall limit. RWM stability is controlled by damping related to plasma rotation relative to the slowly rotating mode structure. Studies of the amplification of externally applied resonant magnetic fields, at β_N above the no-wall limit, give a means of qualifying physics models of this damping, which in-turn is key to determining RWM stability in ITER. Studies in JET, and related joint experiments on DIII-D [35], show that amplification of applied n=1 resonant magnetic fields are in good agreement when geometry differences between JET and DIII-D are taken into account. Furthermore, this amplification agrees reasonably well with a kinetic damping or strong sound wave damping model [36]. Planned future experiments on JET with n=2 resonant magnetic fields are expected to improve discrimination between the damping models. The suitability of these models for ITER, where rotation between the plasma and the mode will be lower, remains to be assessed. A second series of joint JET/DIII-D experiments shows that in both devices, when β_N exceeds the no-wall limit, a similar threshold level of applied magnetic field ($B_{2,1}/B_T \sim 2\times10^{-4}$) at q=2, induces mode locking and consequent magnetic braking, leading to RWM growth [36]. These results highlight the importance of the proposed error field correction system for ITER, for high β operation.

3. First wall power and particle loadings

3.1. ELM power losses

The Type I ELMs associated with the ITER baseline scenario will cause erosion and damage to plasma facing components. Extrapolations from JET show that ELMs on ITER could expel transiently 3-8% of the 350MJ stored energy, depositing 0.6-3.4MJm^{-2} on the divertor targets [37, 38]. Thus, improved characterisation and understanding of ELM transport in the SOL and the consequences for first wall and divertor power loadings are essential. Careful analysis of infra-red thermographic measurements of divertor target ELM energy deposition from a series of discharges with varying ELM

energy losses up to W_{ELM}=1MJ shows clear evidence for a strong asymmetry favouring the inner target (Fig. 10) [39]. Except at the lower ELM energies (W_{ELM}<100kJ), where the data are more scattered, this asymmetry closely follows $E_{ELM,i}/E_{ELM,o}$=2 and thus counteracts, to some extent, the inter-ELM target energy asymmetry which is heavily weighted towards the outer target, particularly at high input power. This behaviour would be very favourable if found on ITER, since it would relax power loads on the outer targets. At present, there is no explanation for this asymmetry, though it is not a function of pedestal collisionality. Similar observations on ASDEX Upgrade indicate that the asymmetries are related to current flow through the divertor targets [40].

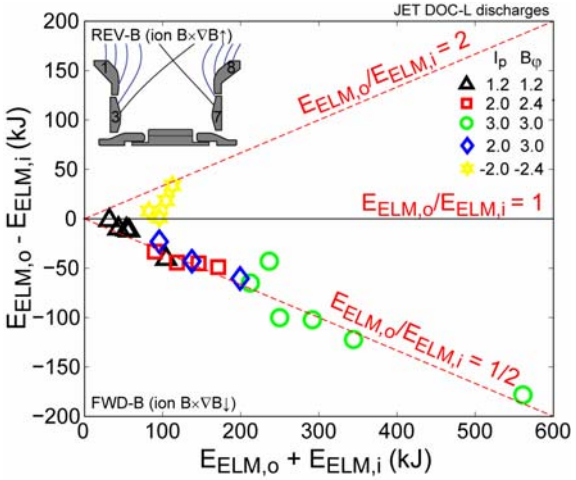

FIG. 10. Energy deposition asymmetry in favour of the inner target during Type I ELMs. I_p and B_φ are in MA and T respectively.

Particle-in-cell simulations of parallel ELM transport under JET-like conditions have been improved considerably over earlier efforts, notably with reduced shortening parameters and increased grid resolution. For a range of W_{ELM}, there are rapid variations in the divertor target sheath heat transmission factors, γ, during the ELM event, particularly for electrons, exceeding classical values by up to 2 orders of magnitude. However, since only about 30% of the ELM energy is carried by the electrons, only at the highest W_{ELM} are the peak target power flux densities significantly over-estimated if, as is common in edge fluid code simulations, γ is assumed constant through the ELM.

A model of the ELM as a series of toroidally rotating, field-aligned filaments is supported by Langmuir probe measurements of plasma flux, T_e and hot ion flux in the far SOL [41]. Further evidence is provided by a new wide angle IR camera system, which has observed helical stripes of power deposition during ELMs on the main chamber and upper dump plate surfaces [39]. Whilst T_e in the ELM filament is lower on reaching the wall than at the pedestal, ions arrive with energies characteristic of the pedestal. This is expected on the basis of a new transient model of ELM filament energy loss which matches probe data in the far SOL, as well as the measured values of the SOL decay lengths during ELMs for prescribed radial propagation velocities [41]. If the latter scale with ELM amplitude, as predicted on the basis of an event driven by interchange motions, the model also reproduces the observed trend on JET for larger ELMs to deposit less energy in the divertor [39].

3.2. Small ELM regimes with plasma shaping

In view of the high power loadings that would result from Type I ELMs in ITER, it is essential to develop the ITER baseline scenario towards one with more benign ELMs. Type III ELMs, such as obtained with impurity injection, are usually accompanied by a reduction in confinement which becomes marginal when extrapolated to ITER and requires further qualification. Plasma shape can also affect ELM behaviour and, in the 2006 quest for intrinsically benign ELMs with high confinement, a stationary regime, which resembles closely the Type II ELMy regime of ASDEX Upgrade, has been produced on JET. This was achieved by matching the plasma shape closely to the quasi-double-null geometry of ASDEX Upgrade, with increased δ_L and decreased δ_U, being possible with the new divertor on JET. Experiments are now underway to resolve the detailed access requirements and behaviour of these benign ELM regimes, testing in particular the role of proximity to double-null, ν^*, β_p and q_{95}. In addition, experiments foreseen for early 2007 will include variation of the Toroidal Magnetic Field Ripple in order to assess its effect on ELMs and confinement [42].

3.3. Material migration and fuel retention

Material migration in the edge of the JET plasma has been inferred from analyses of tiles removed in 2004 (which show strong net deposition on all inner divertor tiles), quartz microbalance (QMB) measurements, and dedicated H-mode experiments in which ^{13}C, injected from the outer divertor, is found in the inner divertor (Fig. 11). This is consistent with upstream transport and SOL flow towards the inner divertor.

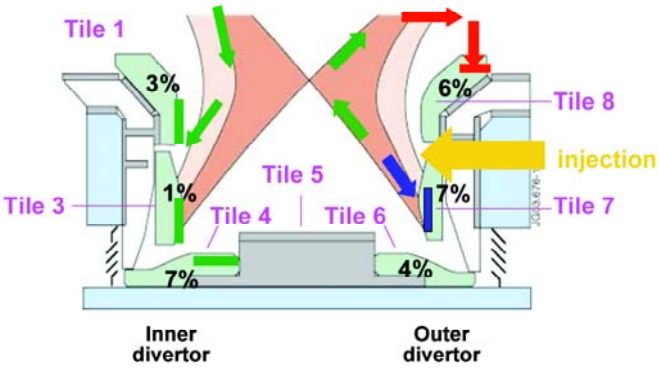

FIG. 11. Material migration and deposition pattern for ^{13}C injected into the outer divertor in a dedicated series of ELMy H-mode discharges.

Material deposition on the inner divertor, evaluated for the first time by metallographic cross-sections of tiles covered originally by 3µm tungsten has been estimated at ~600g, with 60g being in the louvre region and the rest on tile surfaces, corresponding to an average deposition ~7.2mg/s [43, 44]. The layer is 10-70µm thick on Tile 1, up to 300µm on the inclined Tile 4 (due to transport from the strike-point on the inner vertical tiles). The outer vertical tiles, particularly Tile 7, shows heavy erosion. Tile 6 also shows heavy deposition ~380g. Due to surface roughness, the erosion is inhomogeneous over 10-30µm, with adjacent regions showing partial or complete W erosion. Modelling shows that this results from carbon sputtering, with the maximum net erosion of 7µm being in fair agreement with experiment. The total integrated fuel retention in the divertor in co-deposited layers is estimated to be ~42g, compared with an integrated fuel input of 1800g, yielding a 2.7% retention [45]. This is a lower limit since it does not include retention in the main chamber, Tile 5 (to be analysed), or tile gaps [46], but these are not expected to increase retention by more than 50%.

Campaign-integrated data from a QMB removed from the inner divertor louvre region in 2004 and new pulse-resolved data from a poloidal set of QMBs confirm that plasma configuration largely determines material deposition on a QMB. In ELMy H-modes, up to ~$5 \cdot 10^{16}$ C atoms/cm^{2}s are deposited on the inner divertor QMB if the strike-point is located on Tile 4 (direct line-of-sight to QMB), and is significantly lower for L-modes. New data show that the region near Tile 5 is deposition-dominated or erosion-dominated, dependent on whether the strike-point is on Tile 3 (direct line-of-sight to QMB) or Tile 4, consistent with previous experiments. Modelling with the ERO code also shows the importance of the strike-point location for deposition on the QMB. Furthermore, the QMB removed in 2004 shows a pure carbon deposit with a layer density of 0.95g/cm^3 and indicates fuel release due to heating of the QMB crystal.

Immediately prior to the last shutdown ^{13}C-marked $^{13}CH_4$ was injected between Tiles 7 and 8 (Fig. 11) into the outer SOL during 32 consecutive identical Type I ELMy H-mode discharges, which had strike-points on the vertical targets. The ^{13}C deposition shows ~20% on the outer divertor tiles (most just above the strike-point on Tile 7) and ~7% on the inner divertor tiles. ^{13}C was also found on a fast reciprocating collector probe at the top, low-field side of the poloidal cross section, demonstrating material migration around the main plasma from the outer to inner divertor. Transport through the private flux region to Tile 6 and, possibly to Tile 4, was also observed. ^{13}C is not found in the shadow of these tiles, in agreement with QMB data which show transport to such remote areas taking place mainly when the strike-point is on the horizontal target.

EDGE2D modelling of injected ^{13}C shows long-range carbon migration between ELMs which is suppressed during ELMs due to increased divertor temperature, higher ionisation and local re-deposition. The model includes increased transport to simulate ELMs, no carbon re-erosion, and a high SOL flow imposed to match measurements. The modelled ^{13}C deposition indicates that most (98%) of the injected ^{13}C is deposited on the outer target with a few percent reaching the divertor via

the main chamber SOL and the private flux region. The high SOL flows measured are also reproduced by a 2-D electrostatic turbulence code (ESEL) which simulates the observed strongly intermittent turbulent transport. The n_e, T_e and vorticity profiles are evolved together with the fluctuations. Parallel losses in the SOL are described by sub-sonic advection and classical thermal diffusion, while perpendicular fluxes are driven by Pfirsch-Schlueter neoclassical diffusivity. Simulations of ohmic plasmas show that n_e and T_e decay in the SOL faster near the separatrix, in fair agreement with measurements in both near and far SOL. The turbulent fluxes are two orders of magnitude higher than collisional values and, in agreement with measurements, Mach numbers M~0.2 are predicted for the toroidal field independent component of the parallel flows [47].

4. R&D for an ITER-like Wall on JET

In order to test the suitability of the first wall materials foreseen for ITER with regard to power and particle loadings, the installation of an ITER-like Wall is planned on JET. This comprises a full replacement of the first wall with beryllium for the main chamber walls, bulk tungsten for the load bearing septum replacement plate (LBSRP) and tungsten-coated CFC for the remaining divertor tiles. A significant level of R&D has been undertaken in order to select appropriate coatings. 14 different types of W coatings [48], including chemical vapour deposition (CVD; 4, 10, 200μm), physical vapour deposition (PVD; 4, 10μm) and vacuum plasma spraying (VPS; 200μm) have been tested at power loadings from 4MW/m^2 in 6s to 22MW/m^2 in 1.5s. The surviving 9 coatings were exposed to 200 high heat flux pulses. The different and anisotropic thermal expansion between CFC and W often led to cracking perpendicular to the fibres, inducing de-lamination by buckling along the fibres, melting and partial loss of coating. A 200μm VPS coating and a 10μm ion-assisted magnetron sputtered layer behaved best, and these were exposed also to 1000 cycles at 0.35GW/m^2 (in the electron beam facility, JUDITH) to simulate medium-sized ELMs on JET. The minimisation of electromagnetic forces during disruptions and optimisation of mechanical stability drove the design of the bulk W LBSRP tiles and led to the choice of 6mm W lamellae, packed in 4 poloidal stacks and bolted in the toroidal direction with electrical isolating spacers to reduce eddy currents. Each lamella is in direct electrical contact with the support structure to reduce halo current forces and avoid arcing. A prototype has survived 200 cycles with 7MW for 10s and a failure test with 10MW for 14s in which the temperature exceeded 3000^{o}C. There has also been R&D on Be coatings on Inconel tiles to ensure reduced impurity influxes from the inner wall and upper dump plate claddings, and on marker coatings on bulk Be limiters for the assessment of erosion.

5. Summary and Conclusions

JET results since the last IAEA Conference continue to be significant for ITER and re-enforce the planned upgrades foreseen for the JET Facilities, in particular, the power upgrades (ITER-like ICRH antenna and NB, increasing the total input power from ~30MW to ~45MW) and the ITER-like wall. Coordinated multi-machine experiments have provided further insight into the ν^* and β dependencies of global energy confinement, and new scalings produce an improved fit. However, uncertainty in extrapolation to ITER still exists, but this could be reduced with higher power operation, such as planned on JET. A density peaking factor greater than 1.3 is predicted for ITER. This could off-set a lower-than-expected density limit, but increases the likelihood of impurity accumulation. The ITER-like ICRH antenna will permit this scaling to be extended to higher power with lower fuelling, and offers the opportunity to develop further impurity, sawtooth and NTM control for ITER. Temperature profiles are found to be determined largely by thresholds in R/L_T, and the higher temperatures in ITER will be determined even more closely by thresholds. The power upgrades will allow the range of R/L_T to be extended, and its scaling to be studied. New diagnostics, together with precise experiments, have provided insight into the thresholds for Alfvenic instabilities and the consequences for fast particle redistribution, MHD, turbulence stabilisation and wall loading for ITER. Power and diagnostic upgrades will extend understanding and the capability to control fast particle MHD activity and transport losses by localised current drive, concentrating on the key role of rational magnetic surfaces and ExB shear flows in the formation of an ITB. AT and Hybrid operation has been extended to higher power, and

with more benign ELMs. The power upgrades offer the opportunity of entering an ITER-relevant AT regime in which both bootstrap current and fusion performance increase together. New diagnostics and modelling provide insight into the origin and consequences of ELMs. Divertor power asymmetries during ELMs may relax power loads on the outer targets of ITER. Material migration in the edge of ITER is expected to be similar to that on JET, with erosion of the outer divertor, strong parallel flow in the SOL, deposition on the inner divertor, and sensitivity to magnetic configuration. Fuel retention at the level of 3-4% is found on JET under carbon-dominated conditions. All these results re-enforce the need to test ITER wall materials under high performance conditions, as is foreseen in the longer-term JET programme in support of ITER.

6. Acknowledements

This work was performed under EFDA, by the JET EFDA contributors, listed in the Annex. The presenting author would like to acknowledge the work of all EFDA contributors, especially the Task Force Leaders for this period, those working under the auspices of the JET Operation Contract, all collaborators working on JET under International Agreements and S. A. Arshad for his help in preparing this paper.

References

[1] PAMELA, J., et al., Nucl. Fusion **45** (2005) S63-S85.
[2] ITER Physics Basis, Nucl. Fusion **29** (1999) 2368.
[3] PAMELA, J., et al., 17th International Conference on Plasma Surface Interactions in Controlled Fusion Devices, Hefei, China, 2006.
[4] PAMELA, J., et al., 24th Symposium on Fusion Technology, Warsaw, Poland, 2006.
[5] ITER Physics Basis, Nucl. Fusion **39** (1999) 2175.
[6] McDONALD, D., et al., this conference (Paper EX/P3-5).
[7] RYTER, F., et al., in Proc. 33rd EPS Conf. on Plasma Physics, Rome (2006) submitted for publication in Plasma Phys. Control. Fusion.
[8] MANTICA, P. and RYTER, F., Comptes Rendus Physique **7(6)** (2006) 634-649.
[9] RASMUSSEN, J. Juul., et al., in Proc. 33rd EPS Conf. on Plasma Physics, Rome (2006) P1-076.
[10] TALA, T., et al., this conference (Paper EX/P3-16).
[11] ANGIONI, C., et al., in Proc. 33rd EPS Conf. on Plasma Physics, Rome (2006) P1-090.
[12] WEISEN, H., et al., this conference (Paper EX/8-4).
[13] VALOVIC, M., et al., Plasma Phys. Control. Fusion **46** (2004) 1877.
[14] BORRASS, K., et al., Nucl. Fusion **44** (2004) 752.
[15] GIROUD, C., et al., this conference (Paper EX/8-3).
[16] PUIATTI, M. E., et al., Phys. Plasmas 13:042501 (2006).
[17] ANGIONI, C., et al., Phys. Rev. Lett. 96:095003 (2006).
[18] MURARI, A.., this conference (Paper IT/P1-23).
[19] PINCHES, S. D., KIPTILY, V. G., SHARAPOV, S. E., et al., Nucl. Fusion **46** 11 (2006).
[20] WONG, H. V. and BERK, H. L., Phys. Plasmas **5** (1998) 2781.
[21] PORCELLI, F., et al., Plasma Phys. Control. Fusion **38** (1996) 2163.
[22] PORCELLI, F., this conference (Paper EX/P3-5).
[23] ONGENA, J., this conference (Paper EX/P6-9).
[24] IMBEAUX, F., Plasma Phys. Control. Fusion **47** (2005) B179.
[25] CRISANTI, F., this conference (Paper EX/P1-1).
[26] MANTICA, P., Phys. Rev. Lett. 96:095002 (2006).
[27] SHARAPOV, S.E., et al., Nucl. Fusion **46** (2006) S868.
[28] AUSTIN, M.E., et al., Phys. Plasmas **13** (2006) 082502.
[29] GARBET, X., et al., Nucl. Fusion **43** (2003) 973.
[30] CROMBE, K., et al., Phys. Rev. Lett. 95:155003 (2006).
[31] TALA, T., in Proc. 32nd EPS Conf. on Plasma Physics, Tarragona, Spain (2006) ECA 29 P4.044.
[32] LITAUDON, X., this conference (Paper EX/P1-12).

[33] MOREAU, D., this conference (Paper EX/P1-2).
[34] HACQUIN, S., et al., in Proc. 33rd EPS Conf. on Plasma Physics, Rome (2006)
[35] REIMERDES, H., et al., Phys. Plasmas **13** (2006) 056107.
[36] HENDER, T. C., et al., this conference (Paper EX/P8-18).
[37] LOARTE, A.., et al., Phys. Plasmas **11** (2004) 268.8.
[38] LOARTE, A., et al., this conference (Paper IT/P1-14).
[39] PITTS, R. A., this conference (Paper EX/3-1).
[40] EICH, T., et al., to be published in J. Nucl. Mater.
[41] FUNDAMENSKI, W., and PITTS, R. A., Plasma Phys. Control Fusion **48** (2006) 109.
[42] PARAIL, V., et al., this conference (TH/P8-5).
[43] KIRSCHNER, A., et al., this conference (Paper EX/3-5).
[44] COAD, J.P., 17th International Conference on Plasma Surface Interactions in Controlled Fusion Devices, Hefei, China, 2006.
[45] LOARER, T., et al., this conference (Paper EX/3-6).
[46] RUBEL, T., et al., this conference (Paper EX/P4-24).
[47] NAULIN, V., et al., this conference (Paper TH/P6-22).
[48] MAIER, H., et al., this conference (Paper IT/P2-4).

Annex: List of JET-EFDA Contributors

G. Agarici [5] , M. Airila [43] , R. Akers [34] , R. Albanese [24] , A. Alexeev [62] , A. Alfier [23] , A. Alonso [51] , M. Alonso [1] , B. Alper [34] , H. Altmann [34] , D. Alves [1] , G. Ambrosino [24] , V. Amosov [62] , G. Anda [49] , F. Andersson [19] , E. Andersson-Sundén [16] , V. Andreev [58] , P. L. Andrew [34] , Y. Andrew [34] , M. Angelone [22] , C. Angioni [53] , G. Apruzzese [22] , M. Ariola [24] , R. Armstrong [31] , G. Arnoux [5] , S. Arshad [32 , 34] , G. Artaserse [24] , J. F. Artaud [5] , E. Asp [6] , C. V. Atanasiu [60] , G. Atkins [34] , F. Aumayr [12] , M. D. Axton [34] , A. Baciero [51] , R. A. Baker [34] , M. Baldarelli [22] , S. Balme [5] , N. Balshaw [34] , J. W. Banks [34] , Y. F. Baranov [34] , E. Barbato [22] , G. Barlow [34] , I. L. Barlow [34] , M. A. Barnard [34] , R. Barnsley [30] , L. Barrena [51] , V. Basiuk [5] , G. Bateman [52] , P. Batistoni [22] , S. Bäumel [54] , P. Bayetti [5] , L. Baylor [56] , B. Beaumont [5] , P. S. Beaumont [34] , A. Bécoulet [5] , M. Bécoulet [5] , N. Bekris [41] , M. Beldishevski [34] , A. C. Bell [34] , P. S. A. Belo [1] , P. E. Bennett [34] , N. A. Benterman [34] , G. Berger-By [5] , T. Bergkvist [20] , H. Berk [63] , L. Bertalot [22] , B. Bertrand [5] , M. N. A. Beurskens [34] , Ph. Bibet [5] , T. Biewer [56] , M. A. Bigi [34] , M. Bigi [23] , R. Bilato [53] , J. Bizarro [1] , T. R. Blackman [34] , E. Blanco [51] , J. Blum [50] , V. Bobkov [53] , A. Boboc [34] , D. Boilson [31] , T. Bolzonella [23] , G. Bonheure [2] , X. Bonnin [5] , D. Borba [1 , 32] , A. Borthwick [34] , C. Bourdelle [5] , T. Boyce [34] , H. J. Boyer [34] , A. Bozhenkov [37] , G. Bracco [22] , S. Brad [59] , R. J. Brade [34] , J. M. A. Bradshaw [34] , G. C. Braithwaite [34] , B. Bray [42] , B. Breizman [63] , S. Bremond [5] , P. D. Brennan [34] , S. Brezinsek [37] , B. Brichard [4] , R. Bridge [34] , D. Bridi [12] , M. D. J. Bright [34] , F. Briscoe [34] , M. Brix [34] , G. Brolatti [22] , B. Brotas [1] , B. C. Brown [34] , D. P. D. Brown [34] , A. Bruggeman [4] , A. Bruschi [25] , J. Brzozowski [20] , J. Bucalossi [5] , M. A. Buckley [34] , C. Bucur [59] , T. Budd [34] , R. Budney [57] , P. Buratti [22] , P. R. Butcher [34] , R. J. Buttery [34] , R. Cação [1] , G. Calabrò [22] , C. J. Caldwell-Nichols [41] , C. P. Callaghan [34] , P. G. Camp [34] , D. Campbell [33] , D. C. Campling [34] , A. J. Capel [34] , P. J. Card [34] , A. Cardinali [22] , T. Carlstrom [42] , P. Carman [34] , L. Carraro [23] , C. Castaldo [22] , R. Cavazzana [23] , M. Cavinato [23] , M. Cecconello [20] , F. E. Cecil [28] , A. Cenedese [23] , C. Centioli [22] , R. Cesario [22] , C. D. Challis [34] , A. Chankin [53] , I. T. Chapman [34] , Ph. Chappuis [5] , D. J. Child [34] , G. Chitarin [23] , I. Chugonov [47] , S. Cirant [25] , D. Ciric [34] , R. H. Clarke [34] , J. P. Coad [34] , P. A. Coates [34] , V. Cocilovo [22] , S. Coda [6] , R. Coelho [1] , I. Coffey [30] , S. Collins [34] , J. Compan [36] , J. E. Conboy [34] , S. Conroy [16] , N. Cook [34] , S. P. Cook [34] , S. R. Cooper [34] , J. G. Cordey [34] , Y. Corre [5] , G. Corrigan [34] , S. Cortes [1] , D. Coster [53] , G. F. Counsell [34] , M. Cox [34] , S. J. Cox [34] , T. Craciunescu [60] , S. Cramp [34] , F. Crisanti [22] , I. Cristescu [41] , K. Crombe [3] , B. J. Crowley [34] , N. Cruz [1] , L. Cupido [1] , M. Curuia [59] , R. A. Cusack [34] , A. Czarnecka [9] , S. Dalley [34] , E. T. Daly [34] , A. Dalziel [34] , D. Darrow [57] , O. David [26] , N. Davies [34] , J. J. Davis [34] , C. Day [41] , I. E. Day [34] , M. R. de Baar [32 , 35] , H. J. de Blank [35] , E. de La Luna [51] , C. A. de Meijere [35] , J. L. de Pablos [51] , G. De Temmerman [6] , P. C. de Vries [34] , R. De-Angelis [22] , M. De-Benedetti [22] , F. Degli Agostini [23] , L. Delpech [5] , M. Dentan [5 , 32] , A. J. Denyer [34] , R. F. Denyer [34] , G. De-Tommasi [24] , A. De-Vellis [22] , L. Di Pace [22] , G. Dinescu [60] , P. J. Dirken [34] , A. Dnestrovskiy [58] , L. Doceul [5] , S. E. Dorling [34] , A. P. Down [34] , P. T. Doyle [34] , V. Drozdov [34] , N. Dubuit [5] , P. Dumortier [2] , D. Dunai [49] , I. Duran [8] , A. Durocher [5] , F. Durodié [2] , R. Eaton [34] , T. Edlington [34] , A. M. Edwards [34] , D. C. Edwards [34] , D. T. Edwards [34] , P. K. Edwards [34] , Th. Eich [53] , A. Ekedahl [5] , D. Elbeze [5] , A. Elfimov [1] , B. Ellingboe [31] , R. Ellis [57] , C. G. Elsmore [34] , B. Emmoth [15] , S. K. Erents [34] , G. Ericsson [16] , A. Eriksson [19] , L. G. Eriksson [5] , B. Esposito [22] , H. G. Esser [37] , T. Estrada [51] , G. E. Evans [34] , M. Evrard [2] , G. D. Ewart [34] , D. T. Ewers [34] , G. Falchetto [5] , H. Falter [53] , J. G. A. Fanthome [34] , J. W. Farthing [34] , A. Fasoli [6] , H. Faugel [53] , R. C. Felton [34] , C. Fenzi [5] , H. Fernandes [1] , A. Ferreira [1] , J. A. Ferreira [51] , J. Ferreira [1] , J. Ferron [42] , J. A. Fessey [34] , A. Figueiredo [1] , P. Finburg [34] , J. Fink [53] , K. H. Finken [37] , U. Fischer [41] , N. Fitzgerald [31] , C. Fleming [34] , A. Fonseca [1] , R. A. Forrest [34] , R. J. Francis [34] , B. Franel [5] , J. P. Friconneau [26] , D. Frigione [22 , 32] , J. C. Fuchs [53] , K. Fullard [34] , W. Fundamenski [34] , J. Gafert [32 , 53] , R. Galvão [1] , S. Garavaglia [25] , X. Garbet [5] , O. E. Garcia [13] , P. Garibaldi [5] , J. Garner [34] , L. Garzotti [34] , M. Gatu-Johnson [16] , E. Gauthier [5] , J. W. Gaze [34] , D. F. Gear [34] , J. Gedney [34] , S. J. Gee [34] , E. Genangeli [22 , 32] , S. Gerasimov [34] , A. Geraud [5] , L. Giacomelli [16] , C. S. Gibson [34] , S. J. Gilligan [34] , C. G. Gimblett [34] , D. Gin [47] , E. Giovannozzi [22] , C. Giroud [34] , M. Glugla [41] , J. K. Goff [34] , P. Gohil [42] , V. Goloborod'ko [12] , B. Gonçalves [1 , 32] , M. Goniche [5] , A. Goodyear [34] , N. Gorelenkov [57] , G. Gorini [25] , R. Goulding [56] , D. Graham [34] , E. Graham [34] , M. E. Graham [34] , L. Grando [23] , G. Granucci [25] , J. Graves [6] , N. R. Green [34] , H. Greuner [53] , F. S. Griph [34] , C. Grisolia [5] , G. Gros [5] , A. Grosman [5] , G. Grossetti [25] , S. Gruenhagen [41] , M. P. Gryaznevich [34] , K. Guenther [34] , R. Guirlet [5] , J. Gunn [5] , P. Guzdar [45] , L. J. Hackett [34] , S. Hacquin [1] , B. Haist [34] , S. J. Hall [34] , S. P. Hallworth Cook [34] , D. T. Hamilton [34] , R. C. Handley [34] , J. D. W. Harling [34] , M. J. Harvey [34] , T. D.

V. Haupt [34] , N. C. Hawkes [34] , J. H. Hay [34] , P. W. Haydon [34] , I. R. Hayward [34] , D. Heading [34] , P. J. L. Heesterman [34] , W. Heidbrink [57] , J. Heikkinen [65] , P. Helander [34] , C. Hellesen [16] , T. Hellsten [20] , O. N. Hemming [34] , T. C. Hender [34] , V. Hennion [5 , 32] , C. Hidalgo [51] , J. W. Hill [34] , K. Hill [57] , M. Hill [34] , D. Hillis [56] , T. Hirai [38] , M. Hitchin [34] , A. Hjalmarsson [16] , G. T. Hoang [5] , J. Hobirk [53] , J. Hogan [56] , C. H. A. Hogben [34] , G. M. D. Hogeweij [35] , I. C. Hollingham [34] , K. Holmström [20] , D. A. Homfray [34] , G. Honeyands [34] , C. Hopf [53] , B. A. Horn [34] , A. R. Horton [34] , L. D. Horton [53] , A. J. Hoskins [34] , S. P. Hotchin [34] , M. R. Hough [34] , W. Houlberg [56] , D. F. Howell [34] , M. Hron [8] , A. Huber [37] , V. Huber [40] , Z. Hudson [34] , C. C. Hume [34] , A. J. Hunt [34] , C. L. Hunter [34] , T. S. Hutchinson [34] , S. Huygen [2] , G. Huysmans [5] , V. Hynönen [43] , S. Ide [48] , R. Igreja [1] , F. Imbeaux [5] , L. C. Ingesson [33] , P. Innocente [23] , S. Jachmich [2] , G. Jackson [42] , K. Jakubowska [18] , M. Jakubowski [37] , P. V. James [34] , R. J. E. Jaspers [35] , A. Jaun [21] , I. Jenkins [34] , M. A. C. Jennison [34] , H. S. Jensen [41] , C. Jeskins [34] , E. Joffrin [5 , 32] , M. F. Johnson [34] , R. Johnson [34] , T. Johnson [20] , E. M. Jones [34] , G. Jones [34] , H. D. Jones [34] , T. T. C. Jones [34] , C. Jupén [17] , I. Kachtchouk [62] , J. Källne [16] , D. Kalupin [37] , G. Kamelander [12] , R. Kamendje [11 , 32] , S. Karttunen [65] , M. Kaufmann [53] , G. Kaveney [34] , A. S. Kaye [34] , M. J. Kear [34] , D. L. Keeling [34] , D. Kelliher [31] , N. J. Kemp [34] , N. G. Kidd [34] , R. F. King [34] , D. J. Kinna [34] , V. Kiptily [34] , G. Kirnev [58] , N. Kirneva [58] , K. Kirov [53] , A. Kirschner [37] , T. Kiviniemi [43] , A. Klein [55] , M. Knaup [37] , J. Kneidl [53] , H. Kneupner [37] , P. J. Knight [34] , S. J. Knipe [34] , F. Köchl [12] , G. Kocsis [49] , C. Konz [53] , T. Koppitz [39] , A. Korotkov [34] , H. R. Koslowski [37] , V. Kotov [37] , M. D. Kovari [34] , G. Kramer [57] , A. Krasilnikov [62] , A. Kreter [37] , K. Krieger [53] , A. Kritz [52] , S. Krylov [58] , S. Kuhn [12] , W. Kühnlein [36] , M. Kuldkepp [18] , T. Kurki-Suonio [43] , B. Kuteev [58] , R. La Haye [42] , L. Laborde [5] , R. Laesser [33] , N. Lam [34] , P. Lamalle [2] , P. Lang [53] , M. T. Large [34] , J. S. Larsen [13] , J. R. Last [34] , G. Lawrence [34] , K. D. Lawson [34] , M. Laxåback [20 , 32] , R. A. Layne [34] , E. Lazzaro [25] , F. Le Guern [5 , 32] , H. J. Leggate [34] , M. Lehnen [37] , I. Lengar [10] , M. Lennholm [5] , E. Lerche [2] , C. N. Lescure [34] , A. Li Puma [5] , Y. Liang [37] , J. Likonen [65] , J. Linke [38] , S. A. Linstead [34] , A. Lioure [5 , 32] , X. Litaudon [5] , Y.Q. Liu [14] , C. Llewellyn Smith [34] , T. Loarer [5] , A. Loarte [33] , R. C. Lobel [34] , P. J. Lomas [34] , F. D. Long [34] , J. Lönnroth [43] , D. J. Looker [34] , P. Lotte [5] , F. Louche [2] , M. J. Loughlin [34] , A. B. Loving [34] , T. Luce [42] , R. M. A. Lucock [34] , C. Lungu [60] , A. Lyssoivan [2] , J. Maagdenberg [2] , J. MacGregor [34] , P. Macheta [34] , A. S. Mackenzie [34] , M. Macrae [34] , G. Maddaluno [22] , G. P. Maddison [34] , J. Madsen [13] , P. Maget [5] , C. Maggi [53] , R. Magne [5] , H. Maier [53] , J. Mailloux [34] , M. Makowski [42] , C. J. Manning [34] , M. Mansfield [31] , M. E. Manso [1] , P. Mantica [25] , M. Mantsinen [43] , M. Maraschek [53] , M. A. Marchitti [24] , J. L. Marechal [5] , A. Marinoni [6] , J. Märki [6] , D. Marocco [22] , C. A. Marren [34] , D. L. Martin [34] , D. Martin [34] , Y. Martin [6] , K. Masaki [48] , M. Maslov [6] , A. Matilal [34] , M. Mattei [24] , G. F. Matthews [34] , A. Maviglia [24] , C. R. May [34] , M. Mayer [53] , M. L. Mayoral [34] , D. Mazon [5] , C. Mazzotta [22] , E. Mazzucato [57] , P. McCarthy [31] , K. G. McClements [34] , K. McCormick [53] , P. A. McCullen [34] , D. McCune [57] , D. C. McDonald [34] , J. P. Mckivitt [34] , A. G. Meigs [34] , M. Menard [42] , L. Meneses [1] , S. Menmuir [18] , I. R. Merrigan [34] , Ph. Mertens [37] , A. Messiaen [2] , A. G. Miller [34] , S. F. Mills [34] , J. J. Milnes [34] , F. Mirizzi [22] , R. Mitteau [5] , J. Mlynar [8 , 32] , P. Mollard [5] , I. Monakhov [34] , L. Moneira [34] , P. Monier-Garbet [5] , R. Mooney [34] , D. Moreau [5 , 32] , Ph. Moreau [5] , P. D. Morgan [34] , A. W. Morris [34] , J. Morris [34] , G. L. Mort [34] , C. Mrozek [32 , 53] , A. Mueck [6] , A. Murari [23] , D. Murdock [33] , F. Nabais [1] , E. Nardon [5] , G. Nash [34] , V. Naulin [13] , M. F. F. Nave [1] , R. Nazikian [57] , I. Nedzelski [1] , C. R. Negus [34] , G. F. Neil [34] , J. D. Neilson [34] , A. Neto [1] , R. Neu [53] , O. Neubauer [37] , G. J. Newbert [34] , K. J. Nicholls [34] , A. Nicolai [37] , L. Nicolas [5] , A. H. Nielsen [13] , P. Nielsen [23] , S. K. Nielsen [13] , M. P. S. Nightingale [34] , M. Nora [43] , H. Nordman [19 , 32] , C. Norris [32 , 34] , J-M. Noterdaeme [53] , S. Nowak [25] , I. Nunes [1] , A. Oleynikov [62] , M. O'Mullane [29] , J. Ongena [2 , 32] , F. Orsitto [22] , M. Ottaviani [5] , K. Paget [34] , J. I. Paley [44] , J. Pamela [5] , R. Panek [8] , A. Panin [37] , A. Pankin [57] , V. Parail [34] , Th. Parisot [5] , A. Parkin [34] , A. Parsloe [34] , B. T. Parsons [34] , R. Pasqualotto [23 , 32] , P. Pastor [5] , B. Patel [34] , R. Paterson [34] , A. T. Peacock [33] , R. J. H. Pearce [34] , B. J. Pearson [34] , I. J. Pearson [34] , L. C. Pedrick [34] , M. A. Pedrosa [51] , R. Pereira [1] , C. Perez von Thun [34] , G. Pereverzev [53] , A. Perevezentsev [34] , V. Pericoli [22] , Y. Perrot [26] , S. Peruzzo [23] , G. Petravich [49] , L. Petrizzi [22] , V. Petrov [62] , V. Petrzilka [8] , V. Phillips [37] , G. Piazza [32 , 41] , F. Piccolo [34] , M. Pillon [22] , S. D. Pinches [34] , T. Pinna [22] , G. Pintsuk [38] , A. Pironti [24] , R. Pitts [6] , A. Pizzuto [22] , V. Plyusnin [1] , N. Pomaro [23] , P. J. Pool [34] , S. Popovichev [34] , C. Portafaix [5] , A. Pospieszczyk [37] , R. Prokopowicz [9] , M. E. Puiatti [23] , K. Purahoo [34] , Th. Pütterich [53] , D. Püttmann-Kneupner [32 , 37] , A. Quercia [24] , E. Rachlew [18] , R. W. Rademaker [32 , 35] , M. S. J. Rainford [34] , D. Raisbeck [34] , K. Rantamäki [65] , J. Rapp [32 , 37] , J. J. Rasmussen [13] , G. Raupp [53] , G. Ravera [22] , G Regnoli [22] , M. Reich [53] , R. Reichle [5] , F. Reis [1] , R. Reiss [5 , 32] , D. Reiter [37] , D. Rendell [34] , T. T. Ribeiro [1] , V. Riccardo [34] ,

F. G. Rimini [5] , M. Riva [22] , J. E. C. Roberts [34] , R. J. Robins [34] , D. S. Robinson [34] , S. A. Robinson [34] , D. W. Robson [34] , G. Rocchi [22] , H. Roche [5] , M. Rödig [36] , A. Rolfe [34] , F. Romanelli [22 , 32] , M. Romanelli [34] , J. Romero [51] , E. Ronchi [16] , S. Rosanvallon [5 , 32] , M. Rosinski [9] , J. Roth [53] , Ch. Roux [5] , M. Rubel [20] , C. Ruset [60] , M. Russell [34] , A. Ruth [31] , L. Ryc [9] , A. Rydzy [22] , F. Ryter [53] , S. Saarelma [34] , F. Sabathier [5 , 32] , R. Sabot [5] , S. Sadakov [37] , P. Sagar [34] , G. Saibene [33] , A. Saille [5] , J. F. Salavy [5] , A. Salmi [43] , R. Salomaa [43] , F. Salzedas [1] , U. Samm [37] , J. Sanchez [51] , S. G. Sanders [34] , S. Sanders [34] , K. Sandland [34] , P. Sandquist [19] , D. E. G. Sands [34] , M. I. K. Santala [43] , Y. Sarazin [5] , F. Sartori [34] , R. Sartori [33] , O. Sauter [6] , A. Savelyev [24] , A. Savtchkov [37] , S. C. Scales [34] , A. Scarabosio [6] , A. Scherber [32 , 53] , G. Schilling [57] , C. Schlatter [6] , V. Schmidt [23] , M. Schneider [5] , M. Scholz [9] , K. Schöpf [12] , B. Schweer [37] , J. Schweinzer [53] , J. L. Segui [5] , M. Seki [48] , L. Semeraro [22] , A. Semerok [27] , F. Serra [1] , M. M. J. Shannon [34] , S. E. Sharapov [34] , S. R. Shaw [34] , A. Shevelev [47] , R. Sievering [39] , C. A. Silva [1] , P. A. Simmons [34] , A. Simonetto [25] , D. Simpson [34] , S. Sipila [43] , A. C. C. Sips [53] , H. Sjöstrand [16] , D. Skopintsev [62] , P. G. Smith [34] , J. Snipes [55] , L. Snoj [10] , S. Snyder [52] , S. Soare [59] , E. R. Solano [51] , C. Soltane [5 , 32] , P. Sonato [23] , A. Sopplesa [23] , J. Sousa [1] , C. B. C. Sowden [34] , C. Sozzi [25] , T. Spelzini [34] , J. Spence [34] , F. Spineanu [60] , P. Spuig [5] , A. Stäbler [53] , R. D. Stagg [34] , M. F. Stamp [34] , V. Stancalie [60] , P. Stangeby [42] , D. E. Starkey [34] , M. J. Stead [34] , A. V. Stephen [34] , A. L. Stevens [34] , J. Stober [53] , R. B. Stokes [34] , D. Stork [34] , J. Strachan [57] , P. Strand [19] , W. Studholme [34] , A. Styles [34] , H. P. Summers [29] , P. Sundelin [20] , E. Surrey [34] , D. J. Sutton [34] , W. Suttrop [53] , J. Svensson [53] , D. Swain [56] , B. D. Syme [34] , I. D. Symonds [34] , A. Szydlowski [9] , F. Tabares [51] , H. Takenaga [48] , T. Tala [65] , A. R. Talbot [34] , C. Taliercio [23] , C. Tame [34] , G. Tardini [53] , M. Tardocchi [25] , G. Telesca [3] , A. O. Terrington [34] , D. Testa [6] , J. M. Theis [5] , J. D. Thomas [34] , P. D. Thomas [34] , P. R. Thomas [5] , V. K. Thompson [34] , A. Thyagaraja [34] , P. A. Tigwell [34] , T. Tiscornia [34] , J. M. Todd [34] , T. N. Todd [34] , M. Z. Tokar [37] , J. M. Travere [5] , W. Treutterer [53] , A. Trkov [10] , M. Tsalas [7] , H. Tsige-Tamirat [41] , E. Tsitrone [5] , D. Tskhakaya jun [12] , A. A. Tuccillo [22] , O. Tudisco [22] , S. Tugarinov [62] , M. M. Turner [31] , S. G. J. Tyrrell [34] , N. Umeda [48] , B. Unterberg [37] , A. J. Urquhart [34] , I. Uytdenhoven [38] , A. P. Vadgama [34] , G. Vagliasindi [22] , M. Valisa [23] , M. Valovic [34] , D. Van Eester [2] , B. van Milligen [51] , G .J. van Rooij [35] , A. Vannucci [1] , C. A. F. Varandas [1] , F. Vasut [59] , J. M. Verger [5] , E. Villedieux [5] , F. Villone [24] , J. E. Vince [34] , G. J. Vine [34] , E. Vitale [22] , M. Vlad [60] , I. Voitsekhovitch [34] , M. Vrancken [2] , K. Vulliez [5] , D. Wagner [53] , A. D. Walden [34] , C. W. F. Waldon [34] , M. Walker [34] , M. Walters [34] , B. Walton [34] , R. Warren [34] , J. Waterhouse [34] , M. L. Watkins [32 , 34] , M. J. Watson [34] , M. W. Way [34] , C. R. Webb [34] , J. Weiland [19] , H. Weisen [6] , M. Weiszflog [16] , R. Wenninger [32 , 53] , A. Werner [54] , A. T. West [34] , E. Westerhof [35] , J. M. Weulersse [27] , B. Weyssow [61] , M. R. Wheatley [34] , A. D. Whiteford [29] , A. M. Whitehead [34] , A. G. Whitehurst [34] , A. M. Widdowson [34] , S. Wiesen [37] , A. Wilson [34] , D. J. Wilson [34] , D. Wilson [34] , H. R. Wilson [64] , H. P. Winter [12] , M. Wischmeier [53] , C. Wittmann [53] , D. M. Witts [34] , R. C. Wolf [37] , V. Yavorskij [12] , J. Yorkshades [34] , C. Young [34] , D. Young [34] , I. D. Young [34] , L. Zabeo [34] , A. Zabolotsky [6] , F. Zacek [8] , R. Zagorski [9] , L. Zakharov [57] , K. D. Zastrow [34] , B. Zefran [10] , W. Zeidner [53] , M. Zerbini [22] , Y. Zhu [46] , O. Zimmermann [37] , V. Zoita [60] , S. Zoletnik [49] , F. Zonca [22] , S. Zweben [57] , W. Zwingman [5]

[1]Associação EURATOM/IST, Centro de Fusão Nuclear, Instituto Superior Técnico, Av Rovisco Pais, 1049-001 Lisbon, Portugal, [2]Association "EURATOM - Belgian State" Laboratory for Plasma Physics Koninklijke Militaire School - Ecole Royale Militaire Renaissancelaan 30 Avenue de la Renaissance B-1000 Brussels Belgium, [3]Association EURATOM-Belgian State, Department of Applied Physics UG (Ghent University) Rozier 44 B-9000 Ghent Belgium, [4]Association EURATOM-Belgian State, Studiecentrum voor Kernenergie - Centre d'Etude de l'Energie Nucléaire Boeretang 200 B-2400 Mol, Belgium, [5]Association EURATOM-CEA, DSM/DRFC, CEA/Cadarache, F-13108 Saint Paul-lez-Durance, France, [6]Association EURATOM-Confédération Suisse, Ecole Polytechnique Fédérale de Lausanne (EPFL), CRPP, CH-1015 Lausanne, Switzerland, [7]Association EURATOM-Hellenic Republic, NCSR "Demokritos"153 10, Agia Paraskevi Attica, Greece, [8]Association EURATOM-IPP.CR, Institute of Plasma Physics AS CR, Za Slovankou 3, 182 21 Praha 8, Czech Republic, [9]Association Euratom-IPPLM Hery 23, 01-497 Warsaw, Poland, [10]Association EURATOM-MHST, Jozef Stefan Institute, Reactor Physics Department, Jamova 39, SI-1000 Ljubljana, [11]Association EURATOM-ÖAW, Institut für Theoretische Physik-Computational Physics, Technische Universität Graz, Petersgasse 16, A- 8010 Graz, Austria, [12]Association EURATOM-Österreichische Akademie der Wissenschaften (ÖAW), Austria, [13]Association EURATOM-Risø National Laboratory, Optics and Plasma Research Department, OPL-128, P.O.Box 49, DK-4000 Roskilde, Denmark, [14]Association

EURATOM-VR, Department of Applied Mechanics, Chalmers University of Technology, SE-41296 Gothenburg, Sweden, [15]Association EURATOM-VR, Department of Material Physics, ICT, KTH, SE-16440 Kista, Sweden, [16]Association EURATOM-VR, Department of Neutron Research, Uppsala University, SE-75120 Uppsala, Sweden, [17]Association EURATOM-VR, Department of Physics, Lund University, SE-22100 Lund, Sweden, [18]Association EURATOM-VR, Department of Physics, SCI, KTH, SE-10691 Stockholm, Sweden, [19]Association EURATOM-VR, Department of Radio and Space Science, Chalmers University of Technology, SE-41296 Gothenburg, Sweden, [20]Association EURATOM-VR, Fusion Plasma Physics, EES, KTH, SE-10044 Stockholm, Sweden, [21]Association EURATOM-VR, NADA, CSC, KTH, SE-10044 Stockholm, Sweden, [22]Associazione EURATOM-ENEA sulla Fusione, C.R. Frascati, Roma, Italy, [23]Associazione EURATOM-ENEA sulla Fusione, Consorzio RFX Padova, Italy, [24]Associazione EURATOM-ENEA sulla Fusione, CREATE, Italy., [25]Associazione EURATOM-ENEA sulla Fusione, IFP Milano, Italy, [26]CEA/Fontenay aux Roses, B.P.6 F-92265 Fontenay-aux-roses CEDEX, France, [27]CEA/Saclay, F-91191 Gif-sur-Yvette CEDEX, France, [28]Colorado School of Mines, 1500 Illinois Street, Golden, CO 80401, Colorado, USA, [29]Department of Physics and Applied Physics, University of Strathclyde, Glasgow, G4 ONG, UK, [30]Department of Pure and Applied Physics, Queens University, Belfast, BT7 1NN, UK, [31]Dublin City University (DCU), Ireland, [32]EFDA Close Support Unit, Culham Science Centre, Culham, OX14 3DB, UK, [33]EFDA Close Support Unit, D-85748 Garching, Germany, [34]Euratom/UKAEA Fusion Association, Culham Science Centre, Abingdon, Oxon, OX14 3DB, UK., [35]FOM Institute for Plasma Physics Rijnhuizen, Association EURATOM-FOM, Trilateral Euregio Cluster, The Netherlands, (www.rijnh.nl), [36]Forschungszentrum Jülich GmbH, Fachbereich Betriebsdirektion, D-52425 Jülich, Germany , [37]Forschungszentrum Jülich GmbH, Institut für Plasmaphysik, EURATOM-Assoziation, Trilateral Euregio Cluster, D-52425 Jülich, Germany, [38]Forschungszentrum Jülich GmbH, Institut für Werkstoffe und Verfahren der Energietechnik, EURATOM-Assoziation, D-52425 Jülich, Germany, [39]Forschungszentrum Jülich GmbH, Zentralabteilung Technologie, D-52425 Jülich, Germany, [40]Forschungszentrum Jülich GmbH, Zentralinstitut für Angewandte Mathematik, D-52425 Jülich, Germany, [41]Forschungszentrum Karlsruhe GmbH, P.O.Box 3640, D-76021 Karlsruhe, Germany, [42]General Atomics, P.O.Box 85608, San Diego, CA 92186-5608, California, USA, [43]Helsinki University of Technology, Association EURATOM-Tekes, P.O.Box 4100, FIN-02015 TKK, Finland, [44]Imperial College, University of London, London, SW7 2AZ, UK, [45]Institute for Plasma Research, University of Maryland, College Park, MD 20742-3511, Maryland, USA, [46]Institute of Plasma Physics, Chinese Academy of Sciences Hefei 230031 China, [47]Ioffe Physico-Technical Institute, 26 Politekhnicheskaya, St Petersburg 194021, Russian Federation, [48]Japan Atomic Energy Research Institute, Naka Fusion Research Establishment, Nakamachi, Naka-gun, Ibaraki-ken 311-0913, Japan, [49]KFKI-Research Institute for Particle and Nuclear Physics, Association EURATOM, P.O.Box 49, H-1525, Budapest, Hungary, [50]Laboratoire J.A.Dieudonné, Université de Nice-Sophia-Antipolis, Parc Valrose, F-06108 Nice CEDEX 02, France, [51]Laboratorio Nacional de Fusion, Asociacion EURATOM-CIEMAT, Madrid, Spain, [52]Lehigh University, Bethlehem, PA 18015, Pennsylvania, USA, [53]Max-Planck-Institut für Plasmaphysik, EURATOM-Assoziation, D-85748 Garching, Germany, [54]Max-Planck-Institut für Plasmaphysik, Teilinsitut Greifswald, EURATOM-Assoziation, D-17491 Greifswald, Germany, [55]MIT Plasma Science and Fusion Centre, Cambridge, MA 02139, Massachusetts, USA, [56]Oak Ridge National Laboratory, Oak Ridge, TN 37831-6169, Tennessee, USA, [57]Princeton Plasma Physics Laboratory, James Forrestal Campus, Princeton, NJ 08543, New Jersey, USA, [58]RRC Kurchatov Institute, 1 Kurchatov Square, Moscow 123182, Russian Federation, [59]The National Institute for Cryogenics and Isotopic Technology, Association EURATOM-MEdC, Ramnicu Valcea, Romania, [60]The National Institute for Laser, Plasma and Radiation Physics, Association EURATOM-MEdC, Magurele-Bucharest, Romania, [61]Theoretical and Mathematical Physics, Statistical and Plasma Physics Unit, Association EURATOM-Belgian State, Université Libre de Bruxelles, Campus Plaine, CP 231, Boulevard du Triomphe, B-1050 , [62]Troitsk Insitute of Innovating and Thermonuclear Research (TRINITI), Troitsk 142190, Moscow Region, Russian Federation, [63]University of Texas at Austin, Institute for Fusion Studies, Austin, TX 78712, Texas, USA, [64]University of York, Heslington, York YO10 5DD UK., [65]VTT Technical Research Centre of Finland, Association EURATOM-Tekes, P.O.Box 1000, FIN-02044 VTT, Finland